02

Phonons and features due to ionic conductivity in the reflection spectra of BiF_3 crystal

© A.D. Molchanova[1], S.A. Klimin[1], V.A. Chernyshev[2], K.N. Boldyrev[1], A.R. Valiev[1,3], D.N. Karimov[4]

[1] Institute of Spectroscopy, Russian Academy of Sciences,
108840 Troitsk, Moscow, Russia
[2] Ural Federal University after the first President of Russia B.N. Yeltsin,
620002 Yekaterinburg, Russia
[3] National Research University „Higher School of Economics," Faculty of Physics,
105066 Moscow, Russia
[4] Shubnikov Institute of Crystallography, FSRC „Crystallography and Photonics" RAS,
119333 Moscow, Russia

e-mail: nastyamolchanova@list.ru

Received April 30, 2023
Revised May 04, 2023
Accepted May 08, 2023

Crystals of bismuth fluoride BiF_3 grown from a melt were studied for the first time by optical spectroscopy methods and calculated from first principles in the phonon excitations region. A study of IR reflectance spectra in polarized light was carried out. The parameters of optical phonons were obtained. In the IR reflectance spectra, a low-frequency rise in the range $< 500\,cm^{-1}$, characteristic of conductive materials, is observed. The reflection spectra were analyzed within the framework of the Drude–Lorentz model, taking into account the contribution of ionic conductivity. An *ab initio* calculation of the phonon spectrum of a BiF_3 crystal was carried out and the relationship between theoretical and experimental data was analyzed.

Keywords: IR spectroscopy, BiF_3, *ab initio* calculation of phonon modes, ionic conductivity.

DOI: 10.61011/EOS.2023.09.57340.4941-23

Introduction

Solid electrolytes attract immense interest due to their practical potential. These materials, of which fluorides MF_2 and RF_3 (M and R are di- and trivalent ions of transition metals) are an examples, are used to design solid-state cells, high-value capacitors, and sensors for air contaminants monitoring. Ionic conductivity induces certain low-frequency excitation features in the region of phonon excitations of the lattice. The feasibility of observation of ion plasma oscillations in dynamic conductivity spectra has been considered first in [1]. Features associated with intrinsic excitations of the superionic state, which were interpreted as plasma oscillations, have later been discovered in low-frequency permittivity and reflectance spectra of superionic conductors [2–4]. Since these issues still remain understudied, the examination of phonon spectra of crystals of solid electrolytes is a relevant objective.

Bismuth fluoride BiF_3 (space group $Pnma$, $Z = 4$) is a fluorine ionic conductor [5] and appears to be a viable candidate for application in electrochemistry. BiF_3 is being examined as a compelling conversion-type cathode material for Li-ion batteries due to its high capacity and discharge voltage; according to theoretical predictions, it also undergoes only a minor volume change upon delithiation [6–9]. In addition, BiF_3 and composites based on it are currently the most widely used cathode materials in conversion fluorine-ion batteries [10–13].

In the present study, the phonon spectrum of BiF_3 crystals is examined for the first time via IR reflectance spectroscopy and ab initio calculations in order to identify and perform a symmetry analysis of phonon modes and search for features typical of ionic conductors.

Research methods

Transparent BiF_3 crystals were grown from melt by the Bridgman–Stockbarger method. Ammonium tetrafluorobismutate [14] synthesized in laboratory conditions from commercial high-purity reagents was used as the charge material. The growth proceeded in an active atmosphere of high-purity CF_4.

The results of X-ray diffraction analysis, which was performed using a Rigaku MiniFlex 600 powder diffractometer with CuK_α radiation within the $2\theta = 10°–100°$ angle range, revealed that the obtained BiF_3 crystals are single-phase and crystallize in structural type β-YF_3 (space group $Pnma$ with lattice constants $a = 0.6562$, $b = 0.7014$, and $c = 0.4841\,nm$). Plane-parallel plates oriented along the crystallographic axes were cut out for optical studies.

IR reflectance spectra were recorded at room temperature with a Bruker IFS 125HR Fourier spectrometer fitted with a special reflective attachment. The measurement geometry was close to normal incidence. A polarizer with a wire grid polarized the incident beam in the far IR (FIR,

$10-700\,\mathrm{cm}^{-1}$) spectral region. A pyroelectric deuterated triglycine sulfate (DTGS) detector was used in these measurements. The obtained spectra were approximated within the model of independent harmonic oscillators implemented in RefFIT program [15]. This program uses the least-squares method and performs calculations in accordance with Fresnel equation (1), where frequency-dependent reflection coefficient $R(\omega)$ under normal incidence is expressed in terms of dielectric function $\varepsilon(\omega)$:

$$R(\omega) = \left| \frac{1 - \sqrt{\varepsilon(\omega)}}{1 + \sqrt{\varepsilon(\omega)}} \right|^2. \qquad (1)$$

The complex permittivity may be presented as a sum of N damped oscillators:

$$\varepsilon(\omega) = \varepsilon_\infty + \sum_{j=1}^{N} \frac{f_j \omega_j^2}{\omega_j^2 - \omega^2 + i\gamma_j \omega}. \qquad (2)$$

Here ω_j, f_j , and γ_j are the frequency, the strength, and the damping constant of j-th oscillator and ε_∞ is the high-frequency permittivity.

Calculations were performed within the density functional theory (DFT) with the use of hybrid functionals, which incorporate the contribution of nonlocal exchange in the Hartree–Fock formalism, and non-hybrid functionals in CRYSTAL17 [16,17] (a program developed for modelling of periodical structures within the LCAO-MO approach). An all-electron TZVP basis set [18] was used for fluorine. The inner shells of bismuth were characterized by a relativistic pseudopotential, while its outer shells ($5s^2 5p^6 5d^{10} 6s^2 6p^3$) involved in chemical bonding were characterized by a valence TZVP basis set with diffuse and polarization orbitals [19]. The fluorine basis and the bismuth pseudopotential with the valence basis set are available on the CRYSTAL website [17]. The accuracy of self-consistent field calculation in solving a system of one-electron Kohn–Sham equations was set to 10^{-7} a.u. The accuracy of two-electron integral calculation was no worse than 10^{-8} a.u. Integration over the Brillouin zone was carried out using a $8 \times 8 \times 8$ Monkhorst–Pack k-point grid. The B3PW functional was used in calculation of the phonon spectrum.

Structure and group-theoretical analysis

The primitive orthorhombic cell of a BiF_3 crystal contains four Bi^{3+} ions with eight fluorine F^- ions in the nearest-neighbor environment at a distance of 2.22–2.50 Å at two crystallographic positions in the lattice (Fig. 1) [20,21]. The ninth anion is at a distance of 3.10 Å. This distortion of a Bi^{3+} coordination polyhedron is attributable to it having a stereochemically active lone pair of $6s^2$ electrons. A considerable amount of erroneous data on cubic modification α-BiF_3, which in fact corresponds to high-temperature cubic oxyfluoride BiOF [5,22] that forms due to the fact that bismuth fluoride is prone to pyrohydrolysis, have been published. Under high pressures, BiF_3 assumes the trigonal tysonite structure (space group $P\bar{3}c1$, $Z = 6$) [23].

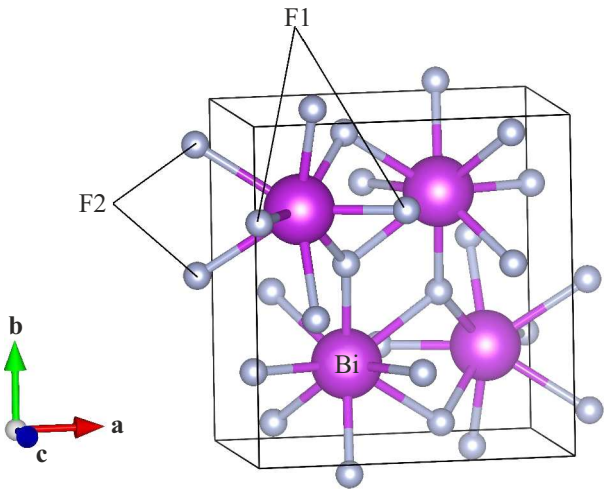

Figure 1. Crystal structure of BiF_3.

The primitive cell of a BiF_3 crystal contains 16 atoms with 48 degrees of freedom, and the crystal itself thus has the same number of normal vibrational modes. Using the data on atomic positions in the structure [20,21], we performed factor group analysis in accordance with [24]. Bi and F1 atoms occupy highly symmetric sites $4c$ [20] and produce modes

$$2A_g + A_u + B_{1g} + 2B_{1u} + 2B_{2g} + B_{2u} + B_{3g} + 2B_{3u}.$$

Atom F2 occupies general site $8d$ and yields modes

$$3A_g + 3A_u + 3B_{1g} + 3B_{1u} + 3B_{2g} + 3B_{2u} + 3B_{3g} + 3B_{3u}.$$

Summing up all these modes and subtracting acoustic ones $B_{1u} + B_{2u} + B_{3u}$, we find the following expression for optical vibrational modes:

$$\Gamma^{\mathrm{vibr}} = 7A_g + 5A_u + 5B_{1g} + 6B_{1u} + 7B_{2g} + 4B_{2u} + 5B_{3g} + 6B_{3u}. \qquad (3)$$

Modes A_u are silent, while the remaining even (gerade) and odd (ungerade) modes are Raman- and IR-active, respectively. It should be stressed that crystals with an inversion center obey the alternative exclusion rule: a vibrational mode cannot be active in both IR and Raman spectra. The following expression holds true for the activity of IR modes in polarized light:

$$\Gamma^{\mathrm{IR}} = 6B_{1u}(\mathbf{E} \parallel z) + 4B_{2u}(\mathbf{E} \parallel y) + 6B_{3u}(\mathbf{E} \parallel x). \qquad (4)$$

The symbols in brackets correspond to allowed components of the electric dipole moment.

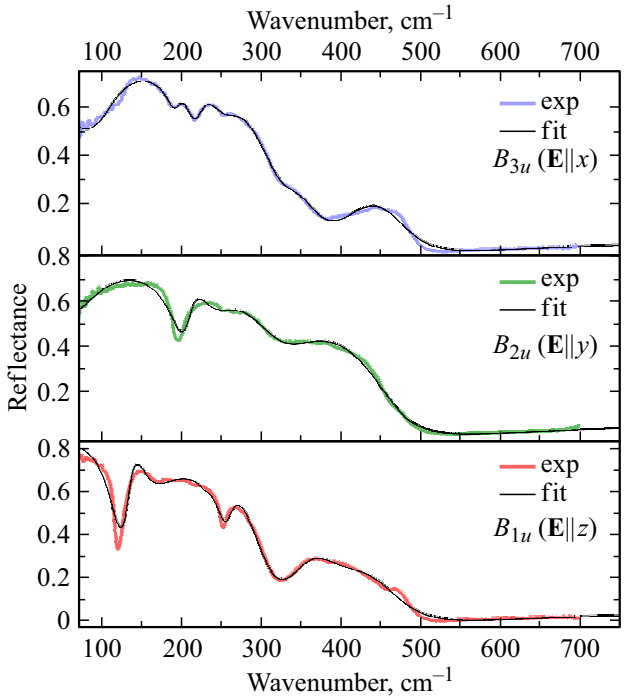

Figure 2. IR reflectance spectra (thick colored curves) of a BiF_3 crystal recorded at room temperature for three different polarizations of incident light ($\mathbf{E} \parallel x$, $\mathbf{E} \parallel y$, $\mathbf{E} \parallel z$). The spectra are compared to fit curves (thin black) plotted using the model of damped oscillators.

Results and discussion

Reflectance spectra measured for polarization directed along each of the crystallographic axes (x, y, z) are shown in Fig. 2. It is evident that the spectra corresponding to three polarizations are widely different. Note that the shape of these spectra differs fundamentally from the usual pattern typical of dielectrics. First, the reflectance increases in the low-frequency region (below $\sim 500\,\mathrm{cm}^{-1}$) in the measured spectra. This is typical for reflection spectra of crystals with free charge carriers (specifically, ionic conductors [25,26]). In BiF_3, the low-frequency reflectance enhancement is likely to be related to the presence of a subsystem of quasi-free F^- anions. Second, phonon modes have an odd shape. They look more like absorption bands or, in certain cases, like inverted phonons. This feature is indicative of the interaction of vibrational modes with the plasma excitation continuum of the subsystem of quasi-free anions.

Assuming that an „ion gas“ similar to electron plasma is present in ionic conductors, one may characterize the contribution of free charges within the model of „quasi-free ions.“ In addition to harmonic oscillators corresponding to common ion oscillations, a Drude oscillator with a zero frequency characterizing the free motion of ions of a disordered sublattice is then included into Eq. (2). Thus,

$$\varepsilon(\omega) = \varepsilon_\infty + \frac{\omega_p^2}{-\omega^2 + i\gamma_p\omega} + \sum_{j=1}^{N} \frac{f_j\omega_j^2}{\omega_j^2 - \omega^2 + i\gamma_j\omega}, \quad (5)$$

where γ_p is the damping constant of an „ionic plasmon“;

$$\omega_p = \sqrt{\frac{4\pi N(Ze)^2}{m\varepsilon}}$$

is the plasma frequency; Z, N, m are the charge, the concentration, and the mass of conduction ions; and ε is the permittivity. Following fitting of the parameters of damped harmonic oscillators and an ionic plasmon, reflectance spectra calculated with the use of permittivity model (5) provide a fine fit to the experimentally measured frequency-dependent reflectance functions (Fig. 2). Thus, all 16 IR-active phonon modes were identified in reflectance spectra, namely, $6B_{1u}$, $4B_{2u}$, and $6B_{3u}$. Their TO frequencies, damping constants, and oscillator strengths were determined in the process of fitting. The B_{1u}, B_{2u}, and B_{3u} phonon parameters are listed in the table.

Plasma frequencies ω_p determined by modeling the reflectance spectra are 404, 552, and 516 cm^{-1} for incident light polarizations $\mathbf{E} \parallel x$, $\mathbf{E} \parallel y$, and $\mathbf{E} \parallel z$, respectively. It was assumed in [3,4] that ion plasma oscillations manifest themselves in optical spectra at frequencies below the frequency ranges of common lattice vibrations. The values of ω_p determined in the present study are several times higher than the minimum phonon frequency observed in IR spectra. A model including both a Drude oscillator with a zero frequency (plasmon) and a so-called relaxator (oscillator with a low TO frequency and a large damping constant) has been proposed earlier for simulation of the dielectric contribution attributable to ionic conductivity [4]. The two corresponding additions produce compensatory contributions to permittivity at low frequencies. However, the introduction of a relaxator necessitates the determination of additional parameters, which cannot be defined unambiguously within the model used here. A more reliable estimate of the contribution of ionic conductivity could be obtained if an estimate of ω_p defined in the following way was known:

$$\omega_p = \sqrt{\frac{4\pi N(Ze)^2}{m\varepsilon}}.$$

However, free carrier concentration N is then needed to calculate the expected plasma frequency value, and it is not possible to deduce this concentration from the available experimental data. Therefore, the contribution of „ion plasma oscillations“ was evaluated only qualitatively.

Ab initio calculations of the phonon spectrum were performed as follows. The crystal structure was optimized first. The calculated lattice constants for BiF_3 were $a = 0.66035$, $b = 0.71206$, and $c = 0.49230$ nm. These values agree closely with the experimental data given above ($a = 0.6562$, $b = 0.7014$, and $c = 0.4841$ nm). The phonon spectrum was then calculated for the optimized

Parameters of IR-active vibrational modes of a BiF_3 crystal: calculated $\omega_{TO,calc}$ (cm^{-1}) and experimental $\omega_{TO,exp}$ (cm^{-1}) TO frequencies, damping constants γ (cm^{-1}) of phonon modes, calculated $\varepsilon_{\infty,calc}$ and experimental $\varepsilon_{\infty,exp}$ high-frequency permittivities, and plasma frequencies ω_p (cm^{-1})

B_{1u}				B_{2u}				B_{3u}			
$\varepsilon_{\infty,exp} = 2.8$, $\varepsilon_{\infty,calc} = 2.97$, $\omega_p = 516$				$\varepsilon_{\infty,exp} = 3.1$, $\varepsilon_{\infty,calc} = 3.14$, $\omega_p = 552$				$\varepsilon_{\infty,exp} = 2.85$, $\varepsilon_{\infty,calc} = 3.2$, $\omega_p = 404$			
$\omega_{TO,calc}$	$\omega_{TO,exp}$	γ	f	$\omega_{TO,calc}$	$\omega_{TO,exp}$	γ	f	$\omega_{TO,calc}$	$\omega_{TO,exp}$	γ^1	f
118	135.8	12.7	2.27	110	102.5	78.7	28.3	110	120.5	51.5	14.2
167	174.5	74	2.55	194	210	22.8	0.7	172	193.6	19.9	0.23
223	230	15	0.02	227	249.9	74.3	0.77	195	221.5	25.4	0.31
257	259.1	22.1	0.13	277	345.6	110.6	0.5	276	256.16	52.2	0.22
342	349.8	62.9	0.34					378	337.1	65.2	0.12
447	409.36	125.1	0.25					416	420.5	86.3	0.30

crystal structure corresponding to the energy minimum. Phonon spectrum frequencies were calculated at the Γ-point. In CRYSTAL, these calculations are performed in the harmonic approximation, and a dynamical matrix is computed in the process. The first and the second derivatives with respect to ion displacements are calculated analytically and numerically, respectively [27]. The obtained data are listed in the Table. It can be seen that the calculated and experimental frequencies agree well for the majority of phonon modes. However, significant deviations are observed for certain modes. This may be attributed to the „mobility" of the fluorine sublattice, which was disregarded in calculations that were carried out under the assumption of an ideal crystal structure of BiF_3. In addition, coupled phonon–plasmon modes can be formed in the case of efficient interaction of certain phonons with plasma oscillations, and the frequencies of these modes may differ greatly from the frequencies of purely phonon excitations [28].

Alongside with TO frequencies, high-frequency permittivities ε_∞ were calculated for three polarizations of incident radiation. The obtained permittivities agree fairly well with the values of ε_∞ determined by modeling the experimental reflectance spectra (see the Table).

Conclusion

The phonon spectrum of BiF_3 (a fluorine ionic conductor) was examined via IR spectroscopy and *ab initio* calculations. IR reflection spectra were recorded for three different polarizations of incident light. The parameters of phonon modes of BiF_3 were determined by modeling the reflection spectra. A fine agreement between experimental and calculated frequencies was obtained for most modes. The differences between frequencies found for certain modes are attributable to the probable manifestation of coupled phonon–plasmon modes in the experiment and the fact that the fluorine sublattice „mobility" was neglected in calculations.

The reflectance enhancement observed in the low-frequency region of spectra is typical of compounds with free charge carriers. The identified feature was interpreted within the Drude−Lorentz model.

Funding

The work of A.D. Molchanova was supported by grant No. 21-72-00134 from the Russian Science Foundation. The work of S.A. Klimin and K.N. Boldyrev was supported by project FFUU 2022-0003 of the Institute of Spectroscopy of the Russian Academy of Sciences. Crystalline samples were grown under the state assignment of the Federal Scientific Research Center „Crystallography and Photonics" of the Russian Academy of Sciences.

Conflict of interest

The authors declare that they have no conflict of interest.

References

[1] J.C. Kimball. Solid State Commun., **32** (11), 1025 (1979). DOI: 10.1016/0038-1098(79)90821-4
[2] T. Awano. Phys. Technol., **51** (5), 458 (2008). DOI: 10.1016/j.infrared.2007.12.018
[3] A.A. Volkov, Yu.G. Goncharov, G.V. Kozlov, G.I. Mirzoyants, A.M. Prokhorov. Dokl. Akad. Nauk SSSR, **284** (4), 846 (1986) (in Russian).
[4] T. Awano, T. Nanba, M. Ikezawa. Solid State Ion., **53–56**, 1269 (1992). DOI: 10.1016/0167-2738(92)90324-i
[5] D.N. Karimov, N.I. Sorokin. Crystallogr. Rep., **68** (2), 297 (2023). DOI: 10.1134/S1063774523020189
[6] J.F. Baumgärtner, F. Krumeich, M. Wörle, K.V. Kravchyk, M.V. Kovalenko. Commun. Chem., **5** (1), 6 (2022). DOI: 10.1038/s42004-021-00622-y

[7] M.F. Oszajca, K.V. Kravchyk, M. Walter, F. Krieg, M.I. Bodnarchuk, M.V. Kovalenko. Nanoscale, **7** (40), 16601 (2015). DOI: 10.1039/c5nr04488j
[8] M. Bervas, F. Badway, L.C. Klein, G.G. Amatucci. Electrochem. Solid-State Lett., **8** (4), A179 (2005). DOI: 10.1149/1.1861040
[9] M. Bervas, A.N. Mansour, W.-S. Yoon, J.F. Al-Sharab, F. Badway, F. Cosandey, L.C. Klein, G.G. Amatucci. J. Electrochem. Soc., **153** (4), A799 (2006). DOI: 10.1149/1.2167951
[10] V.K. Davis, C.M. Bates, K. Omichi, B.M. Savoie, N. Momčilović, Q. Xu, W.J. Wolf, M.A. Webb, K.J. Billings, N.H. Chou, S. Alayoglu, R.K. McKenney, I.M. Darolles, N.G. Nair, A. Hightower, D. Rosenberg, M. Ahmed, C.J. Brooks, T.F. Miller, R.H. Grubbs, S.C. Jones. Science, **362** (6419), 1144 (2018). DOI: 10.1126/science.aat7070
[11] M. Anji Reddy, M. Fichtner. J. Mater. Chem., **21** (43), 17059 (2011). DOI: 10.1039/c1jm13535j
[12] C. Rongeat, M.A. Reddy, T. Diemant, R.J. Behm, M. Fichtner. J. Mater. Chem. A, **2** (48), 20861 (2014). DOI: 10.1039/C4TA02840F
[13] M.A. Nowroozi, I. Mohammad, P. Molaiyan, K. Wissel, A.R. Munnangi, O. Clemens. J. Mater. Chem., **9** (10), 5980 (2021). DOI: 10.1039/d0ta11656d
[14] E.B. Merkulov, A.A. Udovenko, A.B. Slobodyuk. J. Solid State Chem., **314**, 123421 (2022). DOI: 10.1016/j.jssc.2022.123421
[15] A.B. Kuzmenko. Rev. Sci. Instrum., **76** (8), 083108 (2005). DOI: 10.1063/1.1979470
[16] R. Dovesi. CRYSTAL17 User's Manual. [Electronic source]. https://www.crystal.unito.it/Manuals/crystal17.pdf
[17] CRYSTAL17 a computational tool for solid state chemistry and physics. [Electronic source]. http://www.crystal.unito.it/index.php
[18] M.F. Peintinger, D.V. Oliveira, T. Bredow. J. Comput. Chem., **34** (6), 451 (2013). DOI: 10.1002/jcc.23153
[19] E. Heifets, E.A. Kotomin, A.A. Bagaturyants, J. Maier. Phys. Chem. Chem. Phys., **19** (5), 3738 (2017). DOI: 10.1039/c6cp07986e
[20] Von O. Greis, M. Martinez-Ripoll, Z. Anorg. Allg. Chem., **436** (1), 105 (1977). DOI: 10.1002/zaac.19774360112
[21] A.K. Cheetham, N. Norman. Acta Chem. Scand., **28a**, 55 (1974). DOI: 10.3891/acta.chem.scand.28a-0055
[22] M. Kawasaki, H. Kiuchi, K. Shimoda, G. Kano, H. Fujimoto, Z. Ogumi, T. Abe. J. Electrochem. Soc., **167** (12), 120518 (2020). DOI: 10.1149/1945-7111/abad6d
[23] A.V. Novoselova. Zh. Neorg. Khim., **26**, 1727 (1981) (in Russian).
[24] D.L. Rousseau, R.P. Bauman, S.P.S. Porto. J. Raman Spectrosc., **10** (1), 253 (1981). DOI: 10.1002/jrs.1250100152
[25] K. Funke, A. Jost. Berichte Bunsenges. Für Phys. Chem., **75** (5), 436 (1971). DOI: 10.1002/bbpc.19710750508
[26] G.L. Bottger, A.L. Geddes. J. Chem. Phys., **46** (8), 3000 (1967). DOI: 10.1063/1.1841169
[27] F. Pascale, M. Zicovich-Wilson, F. Lopez Gejo, B. Civalleri, R. Orlando, R. Dovesi. J. Comput. Chem., **25** (6), 888 (2004). DOI: 10.1002/jcc.20019
[28] J. E. Maslar, W. S. Hurst, C. A. Wang. J. Appl. Phys., **104** (10), 103521 (2008). DOI: 10.1063/1.3021159

Translated by D.Safin